Density-functional theory of hard-sphere condensation under gravity

Joseph A. Both and Daniel C. Hong
Department of Physics, Lewis Laboratory, Lehigh University, Bethlehem, Pennsylvania 18015
(Received 1 March 2001; published 20 November 2001)

The onset of condensation of hard spheres in a gravitational field is studied using density-functional theory (DFT). We find that the local density approximation yields results identical to those obtained previously using the kinetic theory [Physica A **271**, 192, (1999)], and a weighted density-functional theory gives qualitatively similar results, namely, that the temperature at which condensation begins at the bottom scales linearly with the weight, diameter, and number of layers of particles. We find also that the different DFT approaches give quantitatively different results for the density profiles at low temperatures. In particular, the weighted density-functional approach reveals the layering of hard spheres in the solid regime.

DOI: 10.1103/PhysRevE.64.061105 PACS number(s): 05.20.−y, 51.30.+i, 45.70.−n, 83.80.Fg

I. INTRODUCTION

In a recent paper, one of the authors (D.C.H) [1] proposed that hard spheres in the presence of a gravitational field g undergo a condensation transition, and identified the transition temperature T_c as a function of external parameters, i.e.,

$$T_c = mgD\mu\phi_c/\mu_0, \tag{1}$$

where m and D are, respectively, the mass and diameter of the hard spheres, μ is the dimensionless layer thickness at $T=0$, and μ_0 and ϕ_c are constants that reflect the particular manner in which a system packs upon condensing. (Note that we have set Boltzmann's constant $k=1$ in the above equation and throughout the rest of this work.) It was argued in Ref. [1] that there exists a critical temperature T_c at which the density at the bottom layer becomes the close-packed density. In the theory developed there, this T_c was identified as the temperature below which the derived density profiles could no longer conserve particle number. It was further argued that since the hard spheres cannot be compressed indefinitely, if the temperature is lowered below T_c, then the first layer should remain at the close-packed state, while the particles at the second layer try to compact themselves and thus crystallize. The crystallization then proceeds upward from the bottom layer as the temperature is lowered. This picture was later confirmed by molecular dynamics simulations [2] for monodisperse hard spheres and was extended to the segregation of binary mixtures of hard spheres of different mass and diameters [3].

In the original work [1], the Enskog kinetic equation was used to obtain the density profile of hard spheres under gravity. However, in an attempt to solve a highly nonlinear integrodifferential kinetic equation, it was assumed that the equilibrium velocity distribution function, $f(\mathbf{r},\mathbf{v})$, factorizes into a product of space and velocity dependent parts, i.e., $f(\mathbf{r},\mathbf{v}) = G(\mathbf{r})\phi(\mathbf{v})$ and further that the functional form of $\phi(\mathbf{v})$ is Gaussian, which should be valid for elastic hard spheres. The factorization assumption is an equilibrium ansatz, which states that the configurational statistics are separated out from the kinetics when the system is at equilibrium, so that all the equilibrium quantities can be obtained from the configurational integral of the partition function. The equilibrium state is then the configuration that minimizes the free energy. Indeed, factorization and integration over velocity are in general fundamental results of equilibrium density-function theory (DFT), so we find it necessary to obtain the results of Ref. [1] by DFT methods. We will first employ the simplest form of the density-functional theory known as the local density approximation (LDA), which assumes that the range of interparticle interaction is much smaller than the typical length scale over which $\rho(\mathbf{r})$ varies [4]. We will show that the LDA and the Enskog theories are in fact identical, so that in both methods the condensation temperature is defined as the temperature at which a particular sum rule, to be discussed below, breaks down. Next, we will analyze the problem with a simple weighted density approximation (WDA) [4–7], which takes into account the local variation of the density function. In this approximation, microscopic information is preserved in the density profile; notably the formation of layered structure shows up in the density profile as oscillations. The peak-to-peak distance of this oscillation is approximately the particle diameter. We define in this approximation the condensation temperature to be that temperature at which the local volume density at the bottom of the sample, averaged over a layer which is one particle diameter thick, reaches the simple cubic (in three dimensions) or simple square (in two dimensions) close-packed value. We admit that this definition is somewhat arbitrary, but find that it satisfies our intuitive sense of the meaning of the onset of condensation: condensation begins when the density at the bottom of the sample becomes large. We will demonstrate that the results of both analyses present a picture identical to those presented in Ref. [1]; in particular, we will show how the value μ_0 that appears in Eq. (1) depends on the approximation.

II. LOCAL DENSITY APPROXIMATION

The essence of the LDA is to assume that the system may be divided into small pieces of nearly constant density and then to treat each piece as though it were part of a homogeneous system [4]. Under these assumptions one may write a free energy functional

$$F_{LDA}[\rho]=\int d\mathbf{r}\rho(\mathbf{r})\psi(\rho(\mathbf{r}))+\int d\mathbf{r}\rho(\mathbf{r})U_{ext}(\mathbf{r}), \quad (2)$$

where $\psi(\rho(\mathbf{r}))$ is the Helmholtz free energy per particle in the absence of an external field and U_{ext} is the potential energy per particle due to an external field, such as, gravity. Minimization of this functional under the global constraint that the number of particles is given by

$$N=\int_V d\mathbf{r}\rho(\mathbf{r}) \quad (3)$$

should yield the desired density profile. To be more specific, we define variables for hard spheres of mass m confined in a d-dimensional volume $V=L^{d-1}H$ with L^{d-1} being the cross-sectional area of a $(d-1)$-dimensional plane and H being the height of the container along which the gravitational field is acting. The Helmholtz free energy per particle consists of two terms,

$$\psi(\rho)=\psi_{id}(\rho)+\psi_{exc}(\rho), \quad (4)$$

where ψ_{id} is the ideal gas contribution

$$\psi_{id}(\rho)=T(\ln[\Lambda^d\rho]-1). \quad (5)$$

Note that $\psi_{id}=-T\ln(z^N/N!)$ with the single particle partition function $z=V(2\pi mT)^{d/2}$ [8] and that we have redefined the thermal wavelength $\Lambda\equiv(2\pi mT)^{-1/2}$. Next, ψ_{exc} is the excess contribution to the free energy due to the configurational integral coming from the interactions among particles and is written for the homogeneous liquid as the integral

$$\psi_{exc}=T\int_0^\rho\left(\frac{P}{\rho' T}-1\right)\frac{d\rho'}{\rho'}. \quad (6)$$

The above equation can be derived from the thermodynamic relation, $P=-(\partial F/\partial V)_T$ with the chain rule: $(\partial/\partial V)_T=(\rho^2/N)(\partial/\partial\rho)_T$. Note that $P/\rho T-1$ is the virial sum. To simplify the problem, we make the assumption that ρ varies only in the direction z parallel to the gravitational field and then integrate out the transverse degrees of freedom to yield the free energy per unit area functional,

$$\frac{F_{LDA}[\rho]}{A}\equiv\overline{F}[\rho]$$
$$=\int_0^\infty dz\,\rho(z)\psi_{id}(\rho(z))+\int_0^\infty dz\,\rho(z)\psi_{exc}(\rho)$$
$$+mg\int_0^\infty dz\,\rho(z)z, \quad (7)$$

where $A=L^{d-1}$ is the cross sectional area in the transverse plane. Minimization of the functional under the constraint Eq. (3) yields the Euler-Lagrange equation for the problem

$$\frac{\delta\overline{F}[\rho]}{\delta\rho}=T\ln[\Lambda^d\rho(z)]+\psi_{exc}(\rho)+\rho\frac{d\psi_{exc}}{d\rho}+mgz=\lambda, \quad (8)$$

where we have introduced a Lagrange multiplier λ. The solutions of the Euler-Lagrange equation are necessarily constrained by Eq. (3), which, if we integrate out the transverse directions, takes the form

$$N/A=\int_0^\infty dz\rho(z).$$

If we define a nondimensional density $\phi\equiv\rho D^d$, then we may make the further definition $\phi_c\mu\equiv N/(A/(D^{d-1}))$, where μ then has the meaning of the number of layers in the sample if its particles were close packed at density ϕ_c. Thus μ measures the nondimensional ''depth'' of the sample. Consequently, the constraint satisfied by $\rho(z)$ is

$$\mu\phi_c=D^{d-1}\int_0^\infty dz\rho(z).$$

Further defining $\zeta\equiv z/D$, we see that λ should be determined by the sum rule

$$\mu\phi_c=\int_0^\infty d\zeta\phi(\zeta)=\int_0^{\phi_0}d\phi\zeta(\phi), \quad (9)$$

where ϕ_0 is the density at the bottom of the sample. [The second equality in Eq. (9) was used in Ref. [1] to determine a constant of integration that arose from integrating Eq. (12) below, which was derived in the Enskog theory treatment of the problem. This had the effect of associating, for given m, g, D, and T, a unique value of ϕ_0 to a given value of μ.] Note that the particular shape of the density profile will depend on the functional form of the pressure P or, equivalently, on the functional form of the excess free energy ψ_{exc}. One may use the Enskog pressure for hard disks or a hard sphere equation of state given by a functional form

$$P=\rho T[1+\gamma\rho D^d\chi(\rho)], \quad (10)$$

where $\chi(\rho)$ is the pair correlation function evaluated at contact $(r=D)$, and where $\gamma=\pi/2$ when $d=2$ and $\gamma=2\pi/3$ when $d=3$. Then

$$\psi_{exc}(\rho)=\int_0^\rho\gamma\rho' D^d\chi(\rho')\frac{d\rho'}{\rho'}. \quad (11)$$

Substituting this form of ψ_{exc} into Eq. (8) and taking the derivative with respect to z generates, in our nondimensional variables, the differential equation

$$\frac{d\phi}{d\zeta}+\frac{mgD}{T}\phi=-\gamma\phi\left[\phi\frac{d\chi}{d\zeta}+2\chi\frac{d\phi}{d\zeta}\right], \quad (12)$$

which is precisely the result obtained in Ref. [1]. Thus the equivalence between the LDA and Enskog theory has been shown, and the constant μ_0 that appears in Eq. (1) can also be derived by the density-functional theory in the local density approximation.

To conclude this section we discuss the general method by which we calculate T_c in the LDA/Enskog theory. (A

presentation of results particular to our choices of equation of state to examine this problem may be found in the Appendix.) First, note on physical grounds that for the liquid phase, the density profile $\phi(\zeta)$ in Eq. (9) ought to be a monotonically decreasing function of the height ζ with its maximum value at the bottom. (Indeed, this is what we have found to be the case when we made calculations using particular forms of the equation of state.) Further, the maximum density ϕ_0 (the density at $z=0$) is a function of temperature, too, with the upper bound $\phi_0 \leqslant \phi_c$. Again, this must be true on physical grounds. So, the integral in Eq. (9) can be written as $f(\phi_0)/\beta$, where $\beta = mgD/T$. The particular form of the function $f(\phi_0)$ naturally depends on the approximation. We have found that in both two and three dimensions using particular equations of state, $f(\phi_0)$ is a monotonically increasing function of ϕ_0. Hence, the maximum physically meaningful value the function $f(\phi)$ may assume is at $\phi_0 = \phi_c$, the value of the close-packed density. Thus, we write $f_{max} = f(\phi_c)$. Since β or equivalently T and the layer thickness μ are arbitrary control parameters, the sum rule, Eq. (9), breaks down when $T \leqslant T_c$, where

$$\mu \phi_c = f_{max} T_c / mgD \equiv \mu_0 T_c / mgD, \tag{13}$$

where we have defined $f_{max} \equiv \mu_0$. It is in this way that the LDA/Enskog theory identifies condensation, i.e., the density at the bottom reaching some ϕ_c, with a failure of a sum rule.

At this juncture, we find it appropriate to mention the point made by Levin [9], and in fact widely known to researchers pursuing non-LDA DFT for some time, that reliable information about the fluid-solid coexistence cannot be obtained by the LDA, because of its inability to include the density variations in a highly structured phase (solid). When the Enskog approximation breaks down, one has to either abandon the approximation and search for a better one, or modify the approximation by removing the unphysical results. In the original paper [1], the latter approach was taken; namely, based on physical grounds, the condensed regime was represented by a constant average density, a Fermi rectangle. Then the remaining liquid regime, the tail of the density profile, was described by the Enskog profile, which was linked to the Fermi rectangle at the liquid-solid interface. While the proportionality constant μ_0 in Eq. (1) obtained this way seems to overestimate, and thus while the Enskog equation fails to locate the precise point of the liquid-solid transition, the prediction of its existence and the scaling relation between the critical temperature T_c and external parameters [Eq. (1)] seem to remain true. We discuss below a more elaborate approximation that does take into account local variations in the structured phase that yield substantially lower values for μ_0 (see Fig. 2), which are somewhat close to the values obtained by a mean field theory [2,3].

III. WEIGHTED DENSITY APPROXIMATION

The essence of the WDA, as introduced by Tarazona [4,5] and Curtin and Ashcroft [6] is to recast Eq. (2), the general form of the free energy functional, as

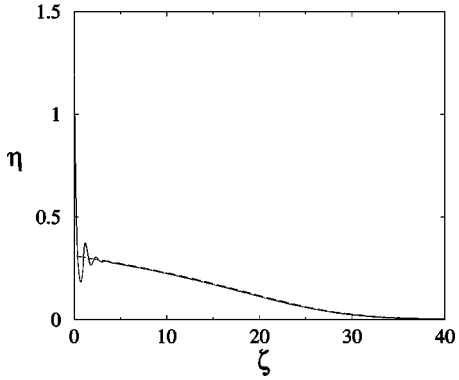

FIG. 1. Solid line is the volume density η as a function of the dimensionless height $\zeta = z/D$ at $T > T_c$ calculated from numerical solution of Eq. (18) for a given set of m, g, D, and μ. The dashed line is the LDA/Enskog profile for the same system at the same temperature.

$$F_{WDA}[\rho] = \int d\mathbf{r} \rho(\mathbf{r}) \psi_{id}(\rho(\mathbf{r})) + \int d\mathbf{r} \rho(\mathbf{r}) \psi_{exc}[\rho_w(\mathbf{r})] + \int d\mathbf{r} \rho(\mathbf{r}) U_{ext}(\mathbf{r}), \tag{14}$$

where $\psi_{exc}[\rho_w(\mathbf{r})]$ is now a functional of $\rho(\mathbf{r})$, depending on $\rho(\mathbf{r})$ through the weighted average of the density given by

$$\rho_w(\mathbf{r}) = \int d\mathbf{r}' w(|\mathbf{r}-\mathbf{r}'|) \rho(\mathbf{r}'), \tag{15}$$

where $w(|\mathbf{r}-\mathbf{r}'|)$ is an appropriately chosen weighting function. Following Tarazona [4], we choose

$$\rho_w(\mathbf{r}) = \frac{3}{4\pi D^3} \int d\mathbf{r}' \Theta(D - |\mathbf{r}-\mathbf{r}'|) \rho(\mathbf{r}'), \tag{16}$$

where Θ is the unit step function, i.e., we replace the local density $\rho(\mathbf{r})$ with its average over a sphere of radius equal to the particle diameter D. Because we assume planar symmetry, i.e., independence in the x and y directions, we may integrate out the transverse degrees of freedom and write explicitly the integral above as a one-dimensional integral,

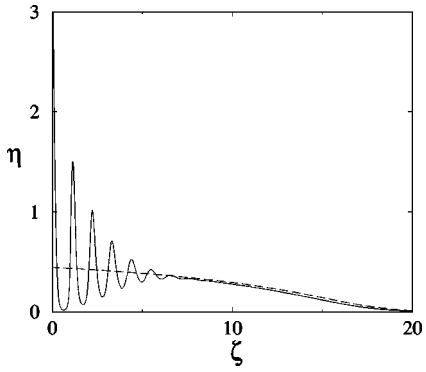

FIG. 2. As in Fig. 1 but with $T \approx T_c$. Note that the vertical range of the graph clips the lowest density peak.

$$\rho_w(z)=\frac{3}{4D^3}\int_0^\infty dz'\rho(z')[D^2-(z-z')^2]\Theta(D-|z-z'|), \tag{17}$$

where $z=0$ corresponds to the position of the center of the particle when its edge is in contact with the bottom wall at $z=-D/2$.

As before, we need to extremize the free energy functional under the global constraint on particle number, so we again use the method of Lagrange multipliers and functional differentiation. Performing the minimization of the free energy functional [Eq. (7) with ρ in the excess term replaced by ρ_w given in Eq. (17)], we find the following equation must hold:

$$T\ln(\Lambda^3\rho)+\psi_{exc}(\rho_w(z))+\int_0^\infty dz'\rho(z')\frac{\delta\psi_{exc}(\rho_w(z'))}{\delta\rho(z)} +mgz+\lambda=0. \tag{18}$$

We write explicitly the integral term in the equation above

$$\int_0^\infty dz'\rho(z')\frac{\delta\psi_{exc}(\rho_w(z'))}{\delta\rho(z)}=\int_0^\infty dz'\rho(z')A(z') \times B(z,z')\Gamma, \tag{19}$$

$$A(z')=\frac{d\psi_{exc}(\rho_w(z'))}{d\rho_w(z')}, \tag{20}$$

$$B(z,z')=[D^2-(z-z')^2]\Theta(D-|z-z'|), \tag{21}$$

$$\Gamma=\frac{3}{4D^3}. \tag{22}$$

The integral equation for $\rho(z)$, Eq. (18), is highly nonlinear and complex and, therefore, requires numerical solution. We choose to solve Eq. (18) using the Carnahan-Starling equation of state, Eq. (A2) (see the Appendix), so that

$$A(z')=-\frac{2}{\rho_w(z')\left[1-\frac{\pi}{6}D^3\rho_w(z')\right]} +\frac{2}{\rho_w(z')\left[1-\frac{\pi}{6}D^3\rho_w(z')\right]^3}. \tag{23}$$

For a given choice of λ we iterate Eq. (18) until the iteration converges to a unique profile. The integral of the profile [Eq. (9)] determines μ, so for fixed m, g, D, and T, we tune λ until the integral of the profile yields the desired number of layers μ. We find that at high temperatures, the profiles obtained using the WDA match very well the profiles obtained for the same set of parameters using the LDA/Enskog approach. But as we lower the temperature of the system, particles at the bottom begin to form dense layers, and the WDA results reflect this by exhibiting oscillations in the density profile near $z=0$. With sufficiently low temperature, the bottom-most peaks in the local density profile grow large and narrow, indicating a greater degree of localization in the dense bottom layers and a tendency toward condensation. However, because our method by itself does not provide a natural and unambiguous way to decide at what point condensation occurs, we are forced to define, with due caution, the critical temperature as the temperature at which the local volume density η at the bottom of the sample, averaged over a layer that is one particle diameter thick (i.e., from $z=-D/2$ to $z=D/2$), reaches the simple cubic (in three dimensions) or simple square (in two dimensions) close-packed value. Figs. 1–3 summarize the development of these density peaks for a representative system from $T>T_c$ through $T<T_c$ and also show the LDA/Enskog results for the same system at the same temperatures. Figure 1 is for $T>T_c$; Fig. 2 is for $T\approx T_c$; Fig. 3 is for $T<T_c$. Note that the peak-to-peak distance of the density oscillations is slightly greater than the diameter of the hard sphere. Note further that our definition of T_c above corresponds qualitatively to another intuitively satisfying interpretation of the onset of condensation: at T_c, the bottom-most density peak is just becoming ''deltalike,'' i.e., this peak and the adjacent one are separated by a region of nearly zero density, while all subsequent peaks are separated by a density substantially greater than zero (see Fig. 2). In contrast, well above T_c the bottom-most layer is not so clearly defined (see Fig. 1), and well below T_c, indeed more than one layer is clearly defined according to this criterion (see Fig. 3). We have found this qualitative correspondence between the integral of the lowest density spike and its approximate degree of localization to hold in both three and two dimensions and independently of the depth of the system. We have, however, not quantified the relationship, and present this remark simply to point out the intuitive reasonableness of our definition of T_c. Finally, note that as T decreases, the WDA and LDA/Enskog density profiles tend to disagree with increasing significance even in the nonoscillatory tails of the profiles (see Fig. 2 and especially Fig. 3).

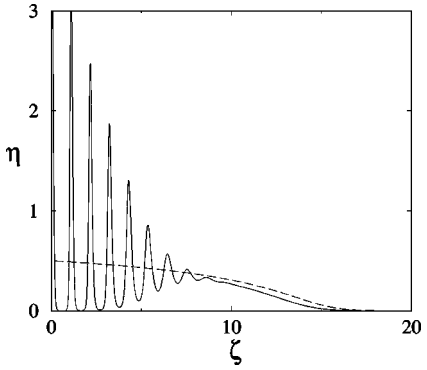

FIG. 3. As in Fig. 1 but with $T<T_c$. Note that the vertical range of the graph clips the lowest two density peaks.

In Fig. 4, for several different sets of m, g, D, we have plotted the dimensionless critical temperature $\tau_c\equiv T_c/mgD$ as a function of the initial layer thickness, μ. The relation-

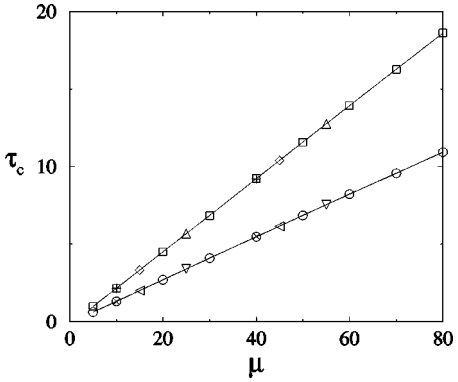

FIG. 4. Dimensionless condensation temperature, $\tau_c \equiv T_c/mgD$, is plotted against the dimensionless layer thickness μ. The slope is $1/\mu_0$. The upper line is for systems with $d=2$, and the lower line is for systems with $d=3$. Different symbols along each line correspond to different sets of *m*, *g*, and *D*.

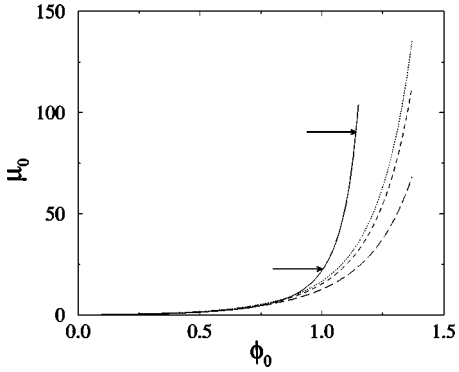

FIG. 5. Value $\mu_0 \equiv f(\phi_0)$ as a function of density at the bottom of the sample ϕ_0 as calculated in the LDA/Enskog theory. The solid curve is for 2D using the Ree and Hoover value of $\chi(\phi)$, Eq. (A3). The remaining curves are for 3D: dotted, Percus-Yevick compressibility form, Eq. (A7); dashed, Carnahan-Starling, Eq. (A4); long dashed, Percus-Yevick virial form, Eq. (A9). The arrows on the 2D curve indicate the range of μ_0 calculated with the LDA/Enskog theory from molecular dynamics simulation values of ϕ_0.

ship turns out to be linear, as predicted in the LDA/Enskog theory as well, and the numerically determined value from the slope for the constant μ_0 is $\mu_0=7.32$ in three dimensions (3D). We have performed an analogous WDA calculation in 2D using the Ree and Hoover correlation function $\chi(\phi)$, Eq. (A1), also for several different sets of *m*, *g*, *D*. The data from this calculation appear in Fig. 2 as well. They yield $\mu_0=4.31$ in 2D. It is important to note that alternate definitions of T_c would lead to slightly different results than those in Fig. 2, but we believe that at the level of the approximations made in this work so far, our results are informative. Both the 2D and 3D WDA results are smaller than those obtained by the LDA/Enskog approach, and we address this next.

As we have discussed, in the LDA/Enskog approach, the value of μ_0 depends on ϕ_0, the density at the bottom, and is identical to the function $f(\phi_0)$. In all the approximations we have used in this work, $f(\phi_0)$ [see Eqs. (A3), (A4), (A7), and (A9)] is a function very sensitive to ϕ_0 for ϕ_0 near close-packed values, i.e., for $\phi_0 \geqslant 1$. Figure 5 illustrates this sensitive dependence. Molecular dynamics simulations in two dimensions [10] have shown that ϕ_0 at $T<T_c$ varies widely. For one set of simulations using 10^3 hard disks with $\mu=20$, defects in packing lead to ϕ_0 occupying the range $1.00<\phi_0<1.14$, with higher densities occurring at lower temperatures. (Note that for square packing in 2D, $\phi_0=1$, while for triangular packing, $\phi_0=2/\sqrt{3}\approx 1.155$.) In LDA/Enskog theory, this range of ϕ_0 leads to $21.76<\mu_0<90.33$ (the arrows in Fig. 5 indicate this range), the large range due to the sensitivity of $f(\phi_0)$, while the WDA theory presented here gives a smaller value, $\mu_0=4.31$ for the 2D calculation using the same equation of state. In the 3D LDA/Enskog calculation using the Carnahan-Starling equation of state, one expects $15.299<\mu_0<152.34$ (the lower bound for simple cubic and the upper bound for hexagonal close packing), while the WDA yields $\mu_0=7.32$. We see that even the lowest possible values that μ_0 may take in the LDA/Enskog approach, namely, those for cubic or square packing (the limit in which comparison to the WDA is most apt, given our definition of T_c in that theory), are indeed greater than those calculated in the WDA theory. Evidently, the LDA/Enskog theory simply predicts lower condensation temperatures than the WDA theory, all other things being equal. To emphasize this difference, we present Fig. 6, which shows for a representative system both the LDA/Enskog and WDA profiles at T_c (LDA), the temperature at which the LDA/Enskog density profile takes the cubic packed density at the bottom ($\phi_0=1$). The dots in Fig. 6 represent the average density of each local maximum, measured between the nearest minima. The three bottom-most peaks have mean density in excess of the cubic close-packed value, and are highly localized. Clearly, at this temperature, the WDA indicates the formation of at least three dense layers, while the LDA/Enskog theory predicts onset of condensation.

Finally, we turn our attention to the question of whether the condensation phenomenon we are considering is a phase transition in the thermodynamic sense, i.e., whether condensation corresponds to a discontinuity in the first or higher derivatives of the free energy with respect to temperature.

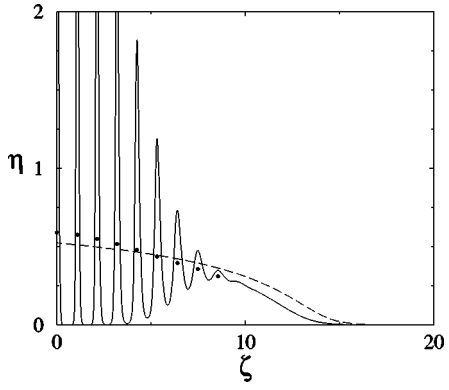

FIG. 6. WDA (solid line) and LDA/Enskog (dashed line) profiles for a representative system at T_c (LDA). The dots are average values of the WDA density peaks. At this temperature, the LDA/Enskog theory indicates onset of condensation, while the WDA theory indicates the formation of at least three dense layers.

We address this question by focusing on the gravitational potential energy contribution to the free energy, $U_g = mg\int_0^\infty z\rho(z)dz$, which is proportional to the center of mass $\langle z\rangle = \int_0^\infty z\rho(z)dz / \int_0^\infty \rho(z)dz$. First we show that in the LDA/Enskog theory, which is extended to temperatures below T_c by the assumption that the density in the frozen layers is given by $\phi = \phi_c$ and that the density above the frozen layers is given by a vertically shifted LDA/Enskog profile [1], a kink in the center of mass develops at $T = T_c$, suggesting a first order transition.

To do this we note that integration of Eq. (12), taken with our previous definitions, shows that the density profile $\phi(\zeta)$ is given by the functional form

$$\beta\zeta = f(\phi) - f(\phi_0), \tag{24}$$

where ϕ_0 is the density at $\zeta = 0$ and $\beta = mgD/T$. Above T_c,

$$\langle\zeta(T)\rangle = \frac{\int_0^\infty \zeta\phi(\zeta)d\zeta}{\int_0^\infty d\zeta\phi(\zeta)} \equiv \frac{1}{\beta} I_1/I_2, \tag{25}$$

where

$$I_1 = \int_{\phi_0(T)}^0 [f(\phi) - f(\phi_0)]\phi\frac{df}{d\phi}d\phi$$

$$I_2 = \int_{\phi_0(T)}^0 \phi\frac{df}{d\phi}d\phi.$$

Now, we note that for T near T_c,

$$\phi_0(T) \approx \phi_c - \alpha(T - T_c), \tag{26}$$

where $\alpha > 0$. Then for any integrand $G(\phi)$ we can make the following approximation:

$$\int_{\phi_0(T)}^0 G(\phi)d\phi \approx \int_{\phi_c}^0 G(\phi)d\phi - \alpha(T - T_c)G(\phi_c). \tag{27}$$

Applying this to the above expression to the integral I_1 and I_2, we find that $\langle\zeta(T)\rangle$ is linear in T with a quadratic correction.

Below T_c, the density profile develops a kink at $\zeta = L$. For $\zeta < L$, $\phi(\zeta) = \phi_c$ the close-packed density, and for $\zeta > L$, the profile is given by the LDA/Enskog profile Eq. (24), and the thickness of the frozen layer is given by [1]

$$L = \mu(1 - T/T_c). \tag{28}$$

We now compute the center of mass $\langle\zeta(T)\rangle$

$$\langle\zeta(T)\rangle = \frac{\int_0^\infty \zeta\phi(\zeta)d\zeta}{\int_0^\infty \phi(\zeta)d\zeta} \equiv \frac{\int_0^L \zeta\phi_c d\zeta + \int_L^\infty \zeta\phi(\zeta - L)d\zeta}{\mu\phi_c}$$

$$\equiv \frac{\phi_c L^2/2 + I}{\mu\phi_c}, \tag{29}$$

where

$$I = \int_0^\infty \zeta\phi(\zeta)d\zeta + L\int_0^\infty \phi(\zeta)d\zeta \equiv I_1 + LI_2$$

$$I_2 = \phi_c(\mu - L). \tag{30}$$

Hence,

$$I = \phi_c\mu^2\frac{T}{T_c}\left(1 - \frac{T}{T_c}\right) + J,$$

where

$$J = \int_0^\infty \zeta\phi(\zeta)d\zeta = \int_{\phi_c}^0 \zeta(\phi)\phi\frac{d\zeta(\phi)}{d\phi}d\phi \equiv \Lambda/\beta^2 \propto T^2$$

and where

$$\Lambda = \int_0^{\phi_c} [f(\phi_c) - f(\phi)]\phi\frac{df(\phi)}{d\phi}d\phi.$$

It, therefore, follows that

$$\langle\zeta(T)\rangle = \frac{\mu}{2} + \lambda_1 T^2, \tag{31}$$

where

$$\lambda_1 = \left[\frac{1}{\mu}\left(\frac{1}{mgD}\right)^2\left(\frac{\Lambda}{\phi_c} - \frac{\mu_0^2}{2}\right)\right].$$

The center of mass scales with temperature quadratically below T_c but linearly just above T_c; thus, there is a kink in the center of mass and in the gravitational potential energy contribution to the free energy, giving rise to a first order transition. The existence of kink in the potential energy at the transition point T_c is in line with the recent rigorous result for one-dimensional hard rods [11].

The scaling of $\langle\zeta\rangle$ with T^2 below T_c survives a modification of how we represent the frozen region. Suppose, the density in the frozen region is not represented by a uniform ϕ_c but is instead given by

$$\phi(\zeta) = \sum_i p_i\delta(\zeta - \zeta_i), \tag{32}$$

where ζ_i is the position of the center of hard spheres and p_i is its peak density in the i-th row forming a crystal. This is a

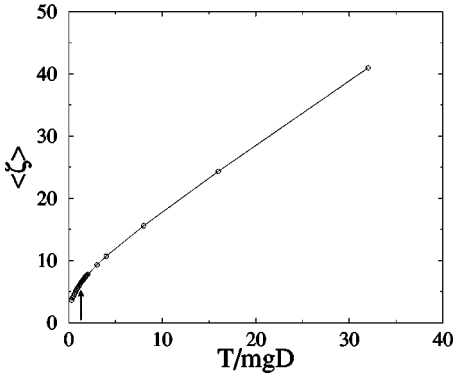

FIG. 7. WDA calculation of center of mass $\langle\zeta\rangle$ vs T/mgD for a system with $\mu=10$. The arrow indicates T_c and points to what may be a kink in the function.

crude way to approximate the oscillations in the density profile due to the crystallization. Then, I_1 in Eq. (30) is replaced by

$$I_1=\int_0^L \zeta\phi(\zeta)d\zeta=\sum_i \zeta_i p_i . \tag{33}$$

If $p_i=\phi_c$ for all i, then,

$$I_1=\phi_c\sum_i \zeta_i=\phi_c[1/2+3/2+5/2+\cdots+(2L-1)/2]$$

$$=\phi_c L^2/2, \tag{34}$$

which is the same result as that obtained by assuming the density profile is approximated by a Fermi rectangle.

The WDA approach to the problem also yields results that may be suggestive of the existence of a first order phase transition. We allow that our method is approximate and that our definition of T_c is open to question, and so a more careful study of the transition in the WDA must be made in future. But it is nonetheless suggestive to examine the dependence of the center of mass $\langle\zeta(T)\rangle$ on T. Figure 7 shows results for a representative system in 3D with $\mu=10$ and whose critical temperature was found to be on the range $1.4mgD<T_c<1.5mgD$. An elbow, possibly a kink, is apparent in the vicinity of T_c, marking the onset of near linear behavior for $T>T_c$. We do not assert that this is evidence of a phase transition; we display this data merely to suggest that the existence of such a phase transition in the WDA approach is not inconsistent with our data. A different form of the weight function in Eq. (15) might yield a better result regarding the nature of the phase transition.

IV. CONCLUSIONS

We have shown that the conclusion of the original paper [1], namely, that the scaling of the critical temperature at which hard spheres under gravity begin to form a solid is linear with their weight, their diameter, and the depth of the sample, necessarily follows from the simplest density-functional theory for the problem (the LDA) and survives a richer density-functional treatment using a WDA. Prudence requires us to note that our WDA for this problem did not include any sophisticated attempt to represent the crystal-fluid interface, something other researchers [12–14] working on similar problems have done. Doing so should likely give a more accurate quantitative picture than that presented here.

ACKNOWLEDGMENT

The authors wish to thank Y. Levin for helpful discussions over the course of this work.

APPENDIX

This appendix contains detailed results from the LDA/Enskog theory. The particular form of the function $f(\phi_0)$, introduced in the local density approximation section, depends on the equation of state chosen to describe the system. Reference [1] [Eq. (15c) and Eq. (16c)] gives the functional forms of ϕ_0 in 2D using the Ree and Hoover correlation function [15];

$$\chi(\phi)=\frac{(1-\alpha_1\phi+\alpha_2\phi^2)}{(1-\alpha\phi)^2}, \tag{A1}$$

$$\alpha=0.489\,351\pi/2,$$

$$\alpha_1=0.196\,703\pi/2,$$

$$\alpha_2=0.006\,519\pi^2/4,$$

and in 3D using the Carnahan-Starling equation of state

$$\frac{P}{\rho T}=\frac{(1+\eta+\eta^2-\eta^3)}{(1-\eta)^3}. \tag{A2}$$

The 2D Ree and Hoover form of $f(\phi_0)$ is given by

$$f(\phi_0)_{RH}=(1+c_2)\phi_0+\frac{1}{2}c_1\phi_0^2+\frac{c_3\phi_0}{(1-\alpha\phi_0)}$$

$$-\frac{c_4}{\alpha}\left(\frac{1}{(1-\alpha\phi_0)}-1\right)+\frac{c_4\phi_0}{(1-\alpha\phi_0)^2} \tag{A3}$$

with $c_1=\pi\alpha_2/\alpha^2\approx 0.0855$, $c_2=-(\pi/2)(\alpha_1/\alpha^2-2\alpha_2/\alpha^3)\approx -0.710$, $c_3=-c_2$, and $c_4=(\pi/2)(1/\alpha-\alpha_1/\alpha^2+\alpha_2/\alpha^3)\approx 1.278$. The 3D Carnahan-Starling form of $f(\phi_0)$ is given by

$$f(\phi_0)_{CS}=\phi_0-\frac{2\phi_0}{(1-\alpha\phi_0)}+\frac{2\phi_0}{(1-\alpha\phi_0)^3}, \tag{A4}$$

where in this expression $\alpha=\pi/6$.

While the scaling of the critical temperature displayed in Eq. (1) is independent of the particular equation of state used in the calculation, the maximum value of $f(\phi_0)$, which we have defined above as μ_0, depends on the functional form of the density profile, or equivalently, the pressure. Using the

two approximations above, and taking the maximum densities as $\eta_c=\pi/6\sqrt{2}\approx 0.74$ in 3D and $\eta_c=\pi/(2\sqrt{3})\approx 0.91$ in 2D, we find

$$\mu_{0RH}=111.31 \quad (2D)$$

$$\mu_{0CS}=152.34 \quad (3D). \tag{A5}$$

At the level of the Enskog approximation, μ_0 is quite sensitive to the density at the bottom, ϕ_0.

In order to show the dependence of μ_0 on approximation, we also compute in it 3D by the Percus-Yevick compressibility form of the equation of state,

$$\frac{P}{\rho T}=\frac{1+\eta+\eta^2}{(1-\eta)^3}, \tag{A6}$$

which yields equally high values for μ_0,

$$f(\phi_0)_{PYC}=\frac{\phi_0}{(1-\alpha\phi_0)}-3\frac{\phi_0}{(1-\alpha\phi_0)^2}+3\frac{\phi_0}{(1-\alpha\phi_0)^3}, \tag{A7}$$

$$\mu_{0PYC}=185.19.$$

The slightly different form, namely, the virial form

$$\frac{P}{\rho T}=\frac{1+2\eta+3\eta^2}{(1-\eta)^2}, \tag{A8}$$

yields

$$f(\phi_0)_{PYV}=3\phi_0-8\frac{\phi_0}{(1-\alpha\phi_0)}+6\frac{\phi_0}{(1-\alpha\phi_0)^2}$$

$$\mu_{0PYV}=86.63. \tag{A9}$$

We further point out that the breakdown of the sum rule is due to the fact that the pressure has a singularity at $\eta=1$, and thus it has a *finite* value at the close-packed density η_c, which is necessarily less than one [8]. If one uses the lattice gas pressure [16],

$$P=-T\ln(1-\rho), \tag{A10}$$

which has a singularity at $\rho=1$, then the condensation temperature is zero, and the density profile is given by the Fermi function [17]

$$\rho(z)=1/\{1+\exp[mg(z-\mu)/T]\}. \tag{A11}$$

[1] D.C. Hong, Physica A **271**, 192 (1999).
[2] P.V. Quinn and D.C. Hong, Phys. Rev. E **62**, 8295 (2000).
[3] D.C. Hong, P.V. Quinn, and S. Luding, Phys. Rev. Lett. **86**, 3423 (2001); see also http://www.nature.com/nsu/010329/010329-1.html; http://www.physicsweb.org/article/news/5/4/5/1
[4] P. Tarazona, Mol. Phys. **52**, 81 (1984).
[5] P. Tarazona, Phys. Rev. A **31**, 2672 (1985).
[6] W.A. Curtin and N.W. Ashcroft, Phys. Rev. A **32**, 2909 (1985).
[7] A. Diehl, M.N. Tamashiro, M.C. Barbosa, and Y. Levin, Physica A **274**, 433 (1999).
[8] J. P. Hansen and I. R. McDonald, *Theory of Simple Liquids* (Academic Press, New York, 1976).
[9] Y. Levin, Physica A **287**, 100 (2000).
[10] P. V. Quinn (private communication).
[11] D.C. Hong, e-print cond-mat/0007494.
[12] R. Ohnesorge, H. Lowen, and H. Wagner, Phys. Rev. A **43**, 2870 (1991).
[13] R. Ohnesorge, H. Lowen, and H. Wagner, Phys. Rev. E **50**, 4801 (1994).
[14] T. Biben, R. Ohnesorge, and H. Lowen, Europhys. Lett. **28**, 665 (1994).
[15] F.R. Ree and W.G. Hoover, J. Chem. Phys. **40**, 939 (1964).
[16] D.C. Hong and K. McGouldrick, Physica A **255**, 415 (1998).
[17] H. Hayakawa and D.C. Hong, Phys. Rev. Lett. **78**, 2764 (1997).